

Moisture dependent wear mechanisms of gallium nitride



Guosong Zeng^{a,b}, Nelson Tansu^{b,c}, Brandon A. Krick^{a,*}

^a Department of Mechanical Engineering and Mechanics, Lehigh University, Bethlehem, PA 18015, USA

^b Center for Photonics and Nanoelectronics, Lehigh University, Bethlehem, PA 18015, USA

^c Department of Electrical and Computer Engineering, Lehigh University, Bethlehem, PA 18015, USA

ARTICLE INFO

Keywords:

Tribochemistry
Wear mechanism
Humidity
GaN

ABSTRACT

Ultralow wear nature of gallium nitride (GaN) has been revealed recently. The wear rate for GaN has a significant dependence on humidity, ranging from $9 \times 10^{-9} \text{ mm}^3/\text{Nm}$ to $9.5 \times 10^{-7} \text{ mm}^3/\text{Nm}$; the mechanisms responsible for this variation in wear remain unclear. Here, we performed reciprocal sliding test on GaN under different environments and characterized the chemical compositions of corresponding worn surface by energy dispersive X-ray spectroscopy (EDS). We show that the surface chemistry of GaN responded differently to various testing environments; this gave rise to the wear rate of GaN spanning over orders of magnitude. Additionally, the EDS conducted on the countersample (alumina probe) clearly evidenced a material transfer from GaN to the ruby countersample. Atomic force microscopy (AFM) and secondary electron microscopy (SEM) inside the wear scar indicated a grooving abrasion wear mechanism of GaN tested under humid environment and adhesive wear mechanism for dry nitrogen testing environment; this is confirmed by SEM/EDS of the ruby probes. In addition, transmission electron microscopy (TEM) was employed to image the defects formed underneath the worn surface, due to the tribological sliding, and the results suggested a possible evolution of wear debris formation.

1. Introduction

Moisture effect on various materials has been studied for decades, including wear of glass [1], and mechanisms of moisture effect on fracture and wear performance of several ceramics, like Si, SiC, Si₃N₄, SiO₂, ZrO, Al₂O₃, GaAs, etc. [2–18] and ceramic filled polymers [19–22]. Wiederhorn published a seminal work on how moisture assisting crack growth on glass and sapphire [1]. He discovered that the measured crack propagation velocity was a function of stress and water vapor concentration. Gee looked into the tribochemical reaction during wear of α -alumina and pointed out that the wear rate of alumina decreased with the increasing of humidity, yet very little effect was found of humidity on friction. It is due to the formation of thin protective/tribochemical films of aluminum hydroxide at the interface [16,18]. Ishigaki et al. performed a pin-on-disk sliding test under various environments, including dry nitrogen, 50% RH and 90% RH, to study the humidity effect on tribological performance (friction and wear) of hot pressed silicon nitride [3]. Their results indicated that the adsorbed water molecules enhanced the plastic flow of silicon nitride and reduced both friction and wear. Fischer and Mullins [10] applied Lewis acid theory to explain the tribochemical reaction occurring during the sliding contact with water vapor presence. They systematically analyzed the tribochemistry of several

representative ceramics, *i.e.*, alumina, silicon nitride, silicon carbide and zirconia, and claimed that the interaction between two ceramics was dominated by charge transfer with ambient environment through acid-base reaction. Erdemir et al. also employed Lewis acid and base and hard and soft acids and bases (HSAB) concepts to help understanding the role of water molecules during tribochemistry on certain solid oxides [11]. Murthy et al. investigated the influence of humidity on friction and wear of silicon carbide [12]. They found that the friction, wear rate and debris size and morphology changed depending on the humidity. Kim's group performed molecular dynamic (MD) simulation to look into the atomistic mechanism of humidity effect on tribochemical wear of silicon oxide [14]. Their results show that the tribochemical reaction occurs at the interface and oxidizes the silicon as a function of adsorbed water molecule amount. It is noteworthy that stress acts as a key role in assisting the chemical reaction [23] and cracking of ceramics under humid environment [24,25]. However, the mechanism of stress corrosion cracking for most of the ceramics still remains unclear [26].

GaN and other III-Nitrides have gained interest as electromechanical materials for numerous device applications [27,28]. These GaN-based devices, including RF-MEMS switches are used under various environments, including desert and space. It is necessary to understand its surface chemical property and wear behavior when interacting with water

* Corresponding author.

E-mail addresses: guz210@lehigh.edu (G. Zeng), tansu@lehigh.edu (N. Tansu), bakrick@lehigh.edu (B.A. Krick).

Table 1
Material properties and working conditions [51,52].

Material Property	Material		Test Condition	
	GaN	α -alumina	Sliding speed	5 mm/s
Young's Modulus	290 ± 5 GPa	350 ± 50 GPa	Relative humidity	Dry nitrogen, 10%, 75%
Poisson's ratio	0.25	0.25–0.3	Normal load	600 mN
Hardness	16 ± 2 GPa	22 ± 3 GPa	Sliding direction	$\langle 1\bar{2}10 \rangle$

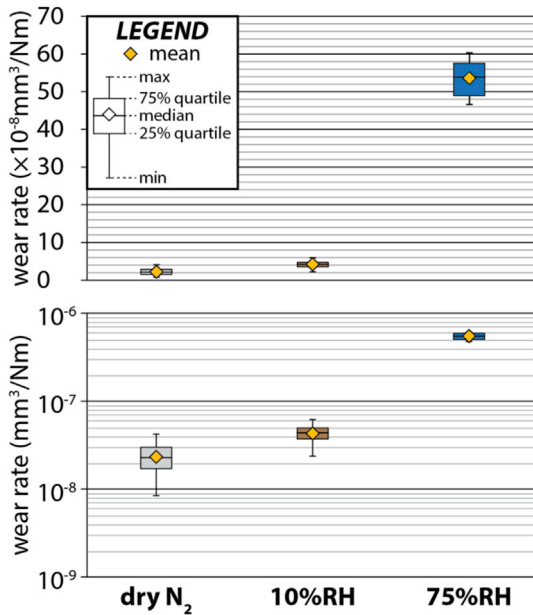


Fig. 1. Wear rate of GaN tested under different environments: dry nitrogen, 10% RH lab air and 75% RH lab air.

molecules, especially under contact condition where stress will be applied. Recently, the ultralow wear nature of GaN has been reported [29], and its wear performance was greatly influenced by humidity. However, the mechanism of humidity effect on GaN wear performance is not fully understood yet. Furthermore, understanding the mechanisms of material removal (e.g. wear, machining and polishing) of GaN surfaces will be relevant for device fabrication and polishing processes [30–32], especially if subtle environmental factors (i.e. humidity) can control material removal rates as well as surface finish and chemistry.

2. Materials and methods

2.1. Materials

Unintentional doped single crystal GaN (3 μm thick) films were grown on c-plane sapphire by metal-organic chemical vapor deposition (MOCVD). The growth of GaN template follows the conventional etch-back and recovery process followed by the high-temperature growth of the n-type layer [33,34]. One MOCVD GaN grown wafer was cut into 4 samples. One sample was used for each environment, and three wear experiments were performed on each sample/environment for repeatability. All the samples are sonicated in acetone and then IPA both for 5 min, and blow the surface dry with ionized dry nitrogen to clean the surface and remove the particles due to sample cutting. Single crystal α -alumina ball (ruby, Swiss Jewel, Grade 25, 1.5 mm diameter) was used as the countersample to reciprocate against GaN coating along $\langle 1\bar{2}10 \rangle$ crystallographic direction as alumina is hard, chemically stable and commonly used as an abrasive material.

2.2. Sliding test

All wear tests were carried out on custom ball-on-flat, reciprocating tribometer mounted inside a glovebox with controlled environment. Testing environments included dry nitrogen (<5 ppm H₂O and <1 ppm O₂), 10% RH ($\pm 5\%$ RH) air, and 75% RH ($\pm 5\%$ RH) air. A cantilever with ruby probe (1.5 mm diameter) attached was used to apply normal load onto the GaN coating. Strain-gauge based biaxial force transducer was used to measure the normal and frictional loads. The applied normal load was kept at $600 \text{ mN} \pm 5 \text{ mN}$ (corresponding to ~ 2 GPa maximum Hertzian contact pressure) in all sliding tests. 2 GPa was chosen to be low enough below hardness to not be doing a scratch test and perform a wear test. Onset of plastic deformation of GaN is ~ 10 – 11 GPa, so 2 GPa is adequately and arbitrarily low enough [35]. A linear motor stage (Aerotech ANT95-L) was employed to achieve the reciprocating sliding. A friction loop consisted of a forward stroke and a reverse stroke. For each reciprocating cycle, friction coefficient was calculated by averaging middle 20% of the friction loop. Material properties and working conditions are summarized in Table 1.

2.3. Wear measurement

Topography of each wear scar was measured by scanning white light interferometry (Bruker ContourGT) to obtain the 3D height profile of the wear scar. The cross-section of the wear scar was extracted from profilometric scan to obtain the cross-sectional area of the lost volume; these were used to measure the Archard wear rate, $K \left[\frac{\text{mm}^3}{\text{N}\cdot\text{m}} \right] = \frac{V[\text{mm}^3]}{F_n[N] \cdot d[\text{m}]}$ (methods discussed in Ref. [36]).

2.4. Surface analysis

Worn surface morphology was analyzed by scanning electron microscopy (SEM, ZEISS 1550) to compare the wear modes for different environments. Energy dispersive X-ray spectroscopy (EDS, Oxford Instruments) was applied to scrutinize the surface composition after the wear test. In addition, atomic force microscopy (AFM) was also employed to measure the microscale surface topography of worn surfaces obtained under all environments.

A TEM specimen was prepared by Ga-source focused ion beam milling (FIB, FEI Scios DualBeam). A 100 nm electron beam assisted platinum followed by 2 μm ion beam assisted platinum were deposited on the worn surface (75% RH testing environment) for surface protection. In order to remove the Ga ion implantation during the milling process, a two-step post-surface-cleaning process was conducted. The specimen was first exposed to the low current Ga ion beam (5 KV, 47 pA), then Ar ion cleaning (Fischione 1040 Nanomill) was performed to further remove the residual Ga ion implantation. Transmission electron microscopy (TEM, JOEL 2000) was utilized to image the defects formed underneath the worn surface for understanding the moisture effect on wear mechanism of GaN.

3. Results and discussion

3.1. Humidity effect on wear performance

The wear rate of GaN ($\langle 1\bar{2}10 \rangle$ direction) strongly depended on the sliding environment (Fig. 1). It can be clearly seen that, from dry nitrogen to 10% RH low humidity lab air, there was only about one-fold increase of the wear rate of GaN, from $K_{\text{nitrogen}} \sim 2.3 \times 10^{-8} \text{ mm}^3/\text{Nm}$ to $K_{10\% \text{ RH}} \sim 4.2 \times 10^{-8} \text{ mm}^3/\text{Nm}$. In stark contrast, the wear rate of GaN in 75% RH air ($K_{75\% \text{ RH}}$) was $\sim 54 \times 10^{-8} \text{ mm}^3/\text{Nm}$, over 20 times higher than the wear in dry nitrogen.

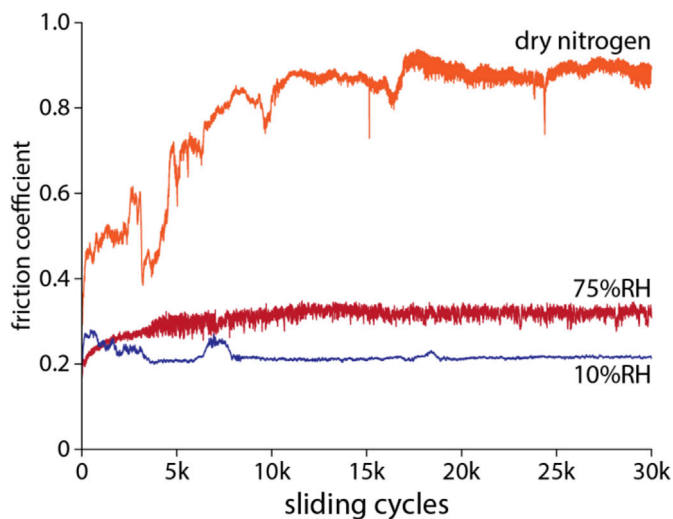


Fig. 2. Friction coefficient of GaN tested under different environments: dry nitrogen, 10% RH lab air and 75% RH lab air.

3.2. Humidity effect on friction

The friction coefficient, μ , provides additional insight into the possible tribochemistry of this system. Fig. 2 shows the averaged friction coefficients vary wildly for the three testing environments. In humid lab air environment (75% RH), the friction coefficients started at ~ 0.15 and gradually went up to ~ 0.3 , where it stabilized at this value for the duration of the test. Low humidity environment is slightly different. For the “run-in” period, the friction coefficient also began with a low value of ~ 0.15 , but went up directly to its highest 0.28, and then dropped back to a lower value of 0.2. Although, there are some increases of friction coefficient occurred during ~ 7000 cycle and $\sim 14,000$ cycle, the friction coefficient remained at ~ 0.2 in the rest of sliding. For dry nitrogen environment, the friction coefficient started at ~ 0.2 and went up to ~ 0.8 – 0.9 in the “run-in” period. Then the friction coefficient remained between 0.8 and 0.9 in the following sliding cycles. The friction versus cycle data in Fig. 2 is characteristic, and general features are verified to

be consistent for multiple experiments ($N \sim 3$ for nitrogen, $N \sim 5$ for 10% RH and $N > 5$ for 75% RH).

The friction results shown in Fig. 2 suggest the water molecules and hydroxyl groups acted as a lubricant at GaN/alumina interface. Much higher frictional force (friction coefficient) in dry nitrogen also indicates a much larger shear stress applied onto the GaN film, and this will correlate to the surface damage and wear mode that will be discussed below. It's noteworthy that, besides the friction coefficient, the “noise” (cycle-to-cycle variation of friction coefficient) of low humidity testing environment during the stable stage is much smaller when compared to dry nitrogen and high humidity environment. This indicates that something other than water molecules or hydroxyl groups formed during sliding for low humidity test, and further decreased and stabilized the friction.

3.3. Surface analysis

The SEM measurement (secondary electron mode) was utilized to image the microscopic morphology of these worn surfaces for wear mechanism comparison. As shown in Fig. 3(a), the worn surface from 75% RH testing environment exhibited a relatively smooth (in the direction of sliding) wear grooves in the surface after 30,000 reciprocating cycles. Both 10% RH [Fig. 3(b)] and dry nitrogen [Fig. 3(c) and (d)] environments had significantly smaller wear scars with less uniform damage features. For 10% RH lab air, small, periodic dark patches were found on the surface [Fig. 3 (b)]. Ridges [Fig. 3(c)] and ridges with potholes [Fig. 3(d)] were found for wear scars from the dry nitrogen testing environment.

The ridges found in the worn surface obtained under dry nitrogen environment after 30,000 reciprocal sliding cycles indicates that the major mechanism of material removal is adhesive wear, *i.e.*, bonding was formed between sample and countersample, and then ruptured by shear stress, which resulted in material transfer from one surface to the other, as well as material fatigue. Furthermore, when the sliding cycles increased to 50,000 cycles, dark potholes were engendered on the surface, as shown in Fig. 3(d). This finding suggests a possible wear debris formation mechanism in dry nitrogen environment, *i.e.*, strong adhesion leads to much higher friction and material fatigue, which eventually causes the material to be knocked out by the ruby probe. Instead, the difference in morphology and defect type from the other two worn

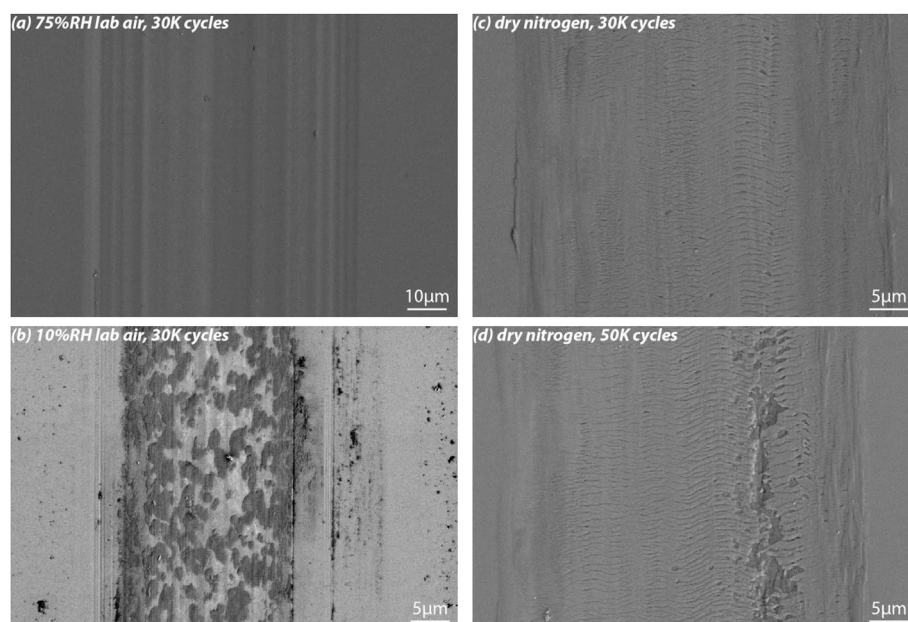


Fig. 3. SEM images of worn surfaces tested under different environments and sliding cycles: (a) 75% RH lab air after 30,000 cycles; (b) 10% RH lab air after 30,000 cycles; (c) dry nitrogen after 30,000 cycles; (d) dry nitrogen after 50,000 cycles.

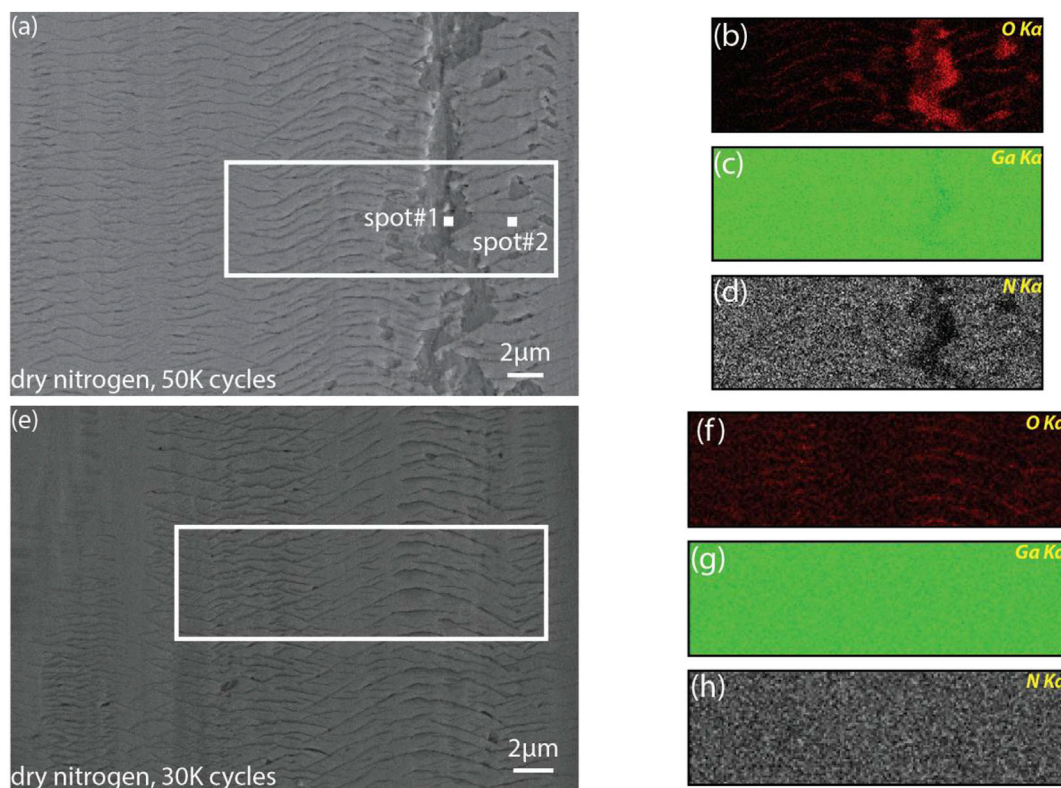


Fig. 4. EDS mapping on worn surfaces: (a–d) dry nitrogen environment after 50,000 cycles: a) SEM, b) O EDS, c) Ga EDS, and d) N EDS., and (e–h) dry nitrogen environment after 30,000 cycles: SEM and EDS mapping on worn surfaces. (a–d) 75% RH lab air environment after 30,000 cycles: (e–h) 10% RH lab air environment after 30,000 cycles: e) SEM, f) O EDS, g) Ga EDS, and h) N EDS.

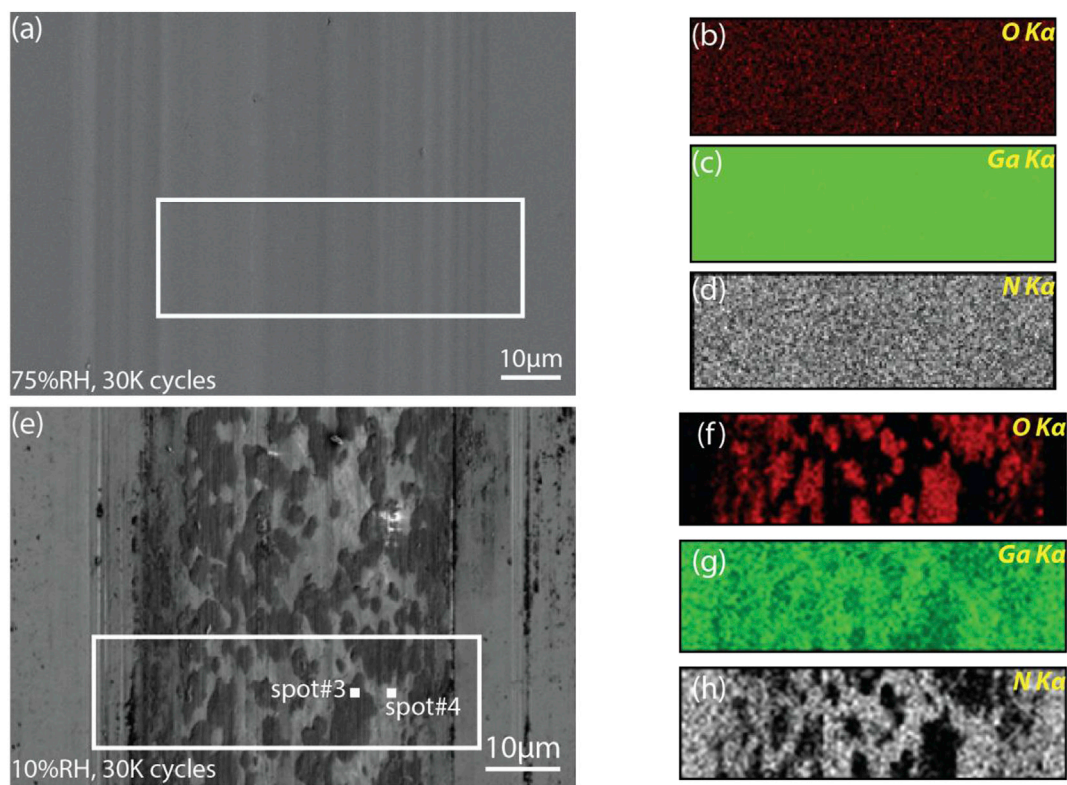


Fig. 5. SEM and EDS mapping on worn surfaces. (a–d) 75% RH lab air environment after 30,000 cycles: a) SEM, b) O EDS, c) Ga EDS, and d) N EDS. (e–h) 10% RH lab air environment after 30,000 cycles: e) SEM, f) O EDS, g) Ga EDS, and h) N EDS. Note: the EDS measurement is more sensitive to Ga, resulting in Ga detection at every pixel in 5c.

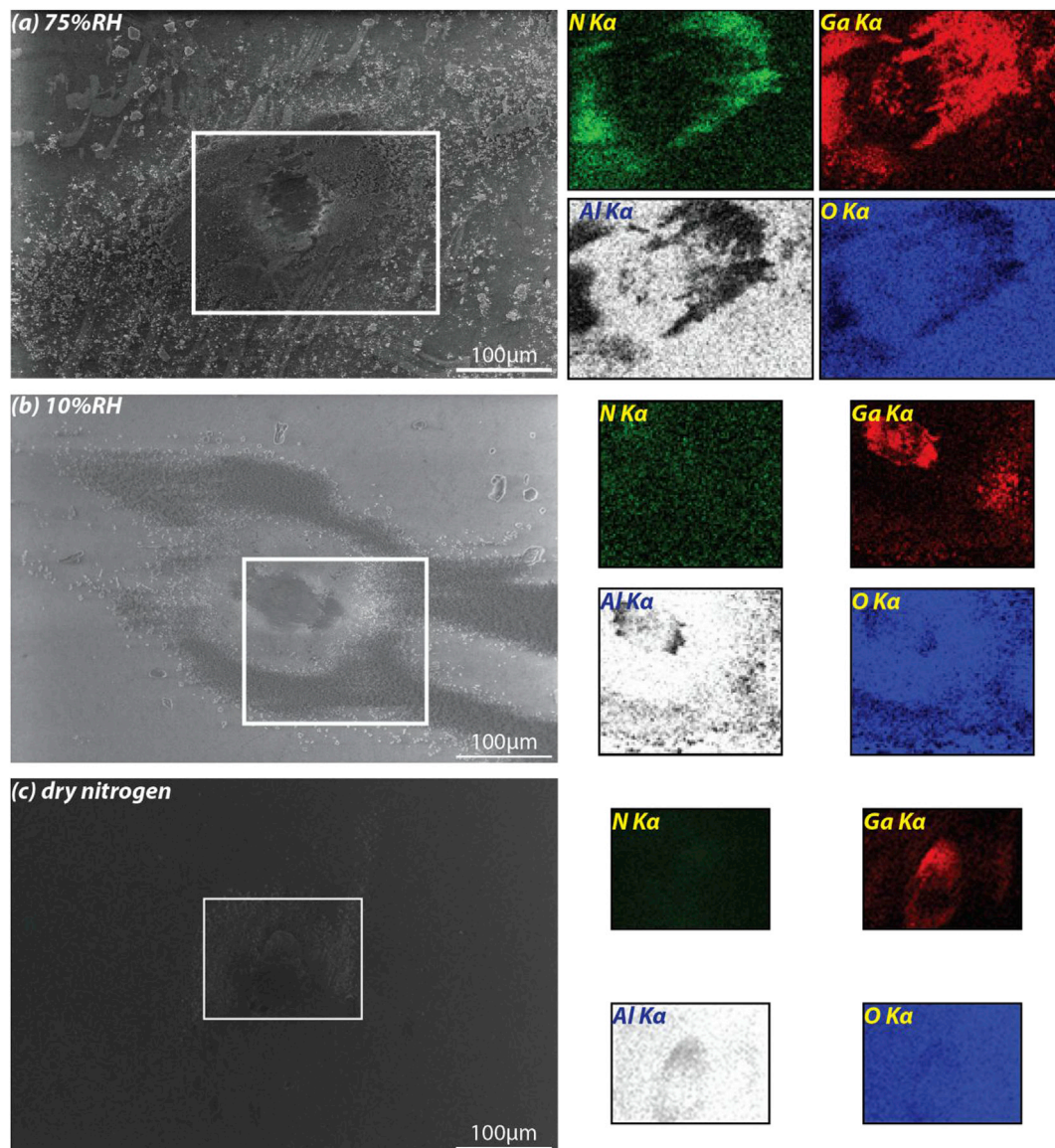


Fig. 6. EDS mapping of N $K\alpha$, Ga $K\alpha$, Al $K\alpha$, and O $K\alpha$ on ruby probes: (a) 75% RH humid environment, (b) 10% RH low humidity environment, and (c) dry nitrogen environment.

surfaces (10% RH and 75% RH) suggests different contact modes in each case. This can arise either from the variation of the shapes of both sample and countersample or the newly formed tribofilms during the wear test.

At 5 kV electron accelerating voltage, the electron penetration is ~ 200 nm in GaN, making EDS surprisingly surface sensitive [35]. Thus, EDS was performed on worn surfaces as well as countersamples to obtain further insight into the tribochemistry for this water-GaN-Alumina tribosystem. From Fig. 4 and Fig. 5, it can be seen that the surface chemical composition revealed by EDS presented different chemical features for each worn surface. Abundant signals of oxygen centered at the ridges and potholes on the worn surfaces were found for dry nitrogen environments while deficient signals of gallium and nitrogen were found at the same area [Fig. 4(a–d)]. The relative intensity ratio of Ga/O for spot#1 and spot#2 are 5.28 and 59.32. Similarly, the ridge patterns on worn surface under dry nitrogen environment obtained after 30,000 cycles also exhibited discernible oxygen signals centering at the ridges [Fig. 4(e–h)]. As reported by Chin et al., a-plane GaN is more susceptible to oxidation than c-plane [37]. Thus, we speculate that the newly formed ridges engendered new planes on the side, e.g., a-plane and m-plane, which are more chemical active than c-plane and easier to be oxidized during the

sample transfer from dry nitrogen environment to SEM chamber, as revealed by EDS.

Counterintuitively, the wear scar obtained from high humidity environment showed indiscernible oxide on the surface based on EDS measurement [Fig. 5(a–d)]. The smoother surface from humid environment (75% RH) consisted of gallium and nitrogen, and a very limited amount of oxygen [Fig. 5(a–d)]. There is likely an oxide layer, however it is too thin for EDS to measure [38]. Density functional theory (DFT) and molecular dynamics (MD) simulations have been intensively applied to investigate the interactions at GaN-water molecule interface [39–42]. It has been shown that the water molecules will dissociate into hydroxyl and hydrogen and bond to Ga and N, respectively, reducing the surface energy. With presence of water molecules, more hydroxyl groups bond to Ga atoms and the surface energy of GaN will be decreased [43]; this can facilitate crack propagation and creation of new surfaces. Furthermore, the ubiquity of defect-induced midgap states in GaN also plays a pivotal role when interacting with water molecules [44]. The thickness of adsorbed water film will increase with the increasing of relative humidity [45]. This humid atmosphere provides a source of oxygen redox couple (acceptors/donors) and thus enhances the charge transfer with midgap

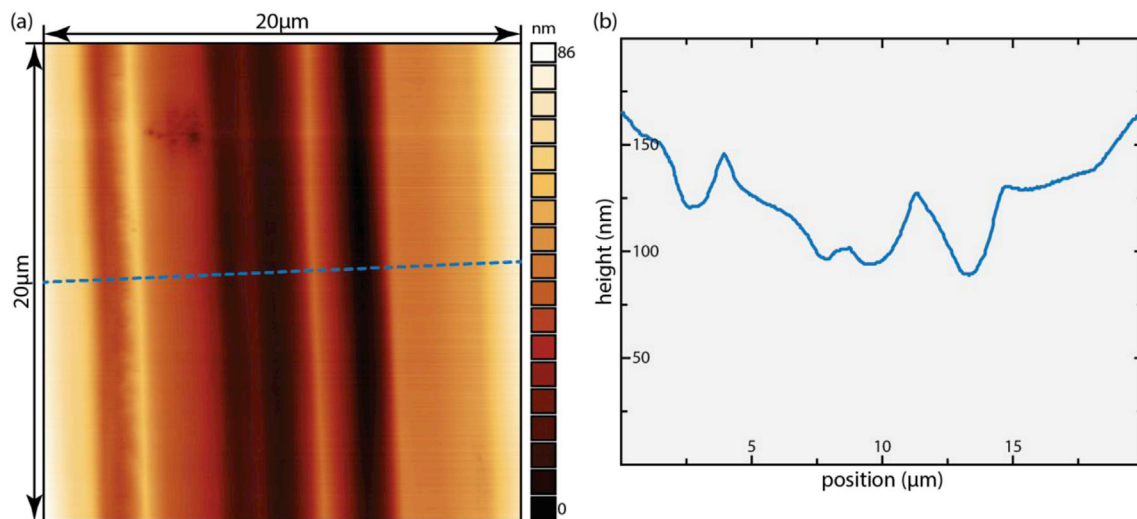


Fig. 7. AFM of GaN wear scar created with 30,000 sliding cycles in 75% RH air. (a) height map. (b) height trace.

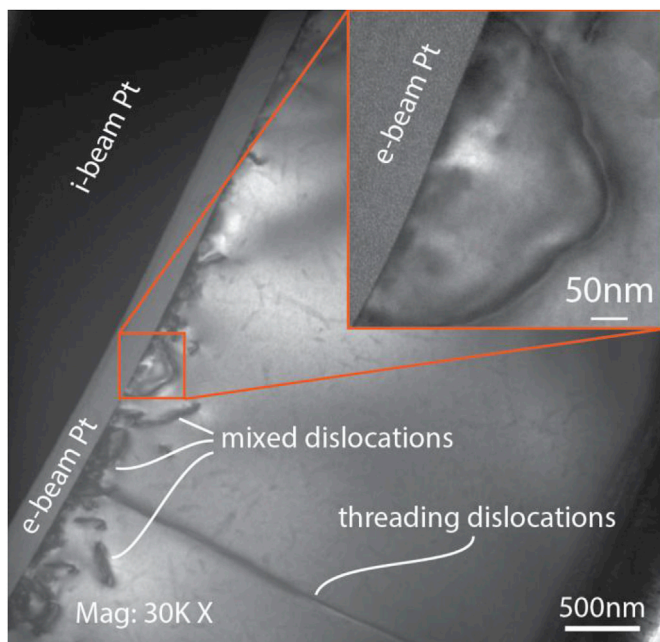


Fig. 8. TEM image of the cross-section of wear scar (75% RH humid environment after 30,000 sliding cycles).

stages of GaN. This will electrochemically pin the Fermi level of GaN and thus assist the oxidation. As a result, generating defects and removing materials from GaN film [as shown in Fig. 3(a)] are much faster. It is noteworthy that there is no Al signal in the EDS, thus EDS maps of Al are not included in Figs. 4 and 5. Furthermore, it was previously observed by scanning Auger microscopy (SAM) that there is no Al in the wear scar [38].

For low humidity environment (10% RH), rich signals of oxygen coming from dark patches at the surface, where less nitrogen signal can be seen [Fig. 5(e–h)]. The relative intensity ratio of Ga/O for spot#3 and spot#4 are 1.22 and 7.45, respectively. This distributed, lubricious oxide layer might be the reason for the low and stable friction we have seen in low humidity environment (Fig. 2). It is noteworthy that by forming these oxide patches, the wear rate of GaN only increased a little but the friction coefficient (~ 0.2) was much lower than the unlubricated dry nitrogen environment (~ 0.8 – 0.9). This might be useful for designs and applications which require both low friction coefficient and ultralow

wear rate.

The ruby probes associated with each wear scar were also examined by SEM and EDS (Fig. 6). It was found that, the ruby probe associated with humid testing environment had a comparable worn surface (~ 60 – $70 \mu\text{m}$ in diameter) with large amount of wear debris (mainly consisted of gallium-oxygen and gallium-nitrogen) surrounding it. This result suggests a two-body grooving abrasive wear mechanism in humid tribosystem for GaN. In contrast, for both dry nitrogen and low humidity testing environments, less wear debris of GaN can be seen. More gallium and nitrogen signals were observed within the contact region on the ruby probe for 10% RH and dry nitrogen experiments, essentially showing a GaN transfer film. Although, the surface damage and tribochemistry for both cases were different, material transfer from GaN to ruby probe present in these two cases. Furthermore, both gallium oxide and gallium nitride were found inside or perhaps just outside the worn area of the ruby probe for low humidity case; this is obviously transfer of third bodies from the wear scar, which consists of both gallium oxide and nitride.

Due to the insufficient height contrast of SEM for humid environment wear scar and the purpose of imaging microscale defects, an AFM scan was performed inside the wear scar to assess the nanoscale topography (where optical interferometry is insufficient). As can be seen in Fig. 7(a), a groove-like profile was presented. Fig. 7(b) shows the profile of a line scan made inside Fig. 7(a), from which we can see that the peak and valley have the lateral size varying from 2 to $7 \mu\text{m}$ and 10–50 nm in depth. The size of the grooves in the wear scar match the size of wear debris accumulated on the ruby probe (Fig. 6a).

To image the defects caused by the sliding contact, a cross-section of the wear scar was prepared by FIB and examined by TEM. Fig. 8 presents the dislocations formed underneath the wear scar which was obtained from humid environment, which is similar to those dislocations formed by nanoindentation on GaN [35,46]. In addition, threading dislocation arising from the lattice mismatch during the epitaxy was also observed [47–49]. The inset of Fig. 8 shows a zoom-in of a dislocation underneath the wear scar. The dislocation appears to wrap from surface to surface with a dimension ($\sim 400 \text{ nm}$) comparable to the size of the wear debris; this indicates a possible mechanism for formation and ejection of wear debris. Induced by the shear stress, the dislocations and cracks will generate and propagate, and both of them directly contribute to the formation of wear debris. The increased humidity is hypothesized to facilitate moisture-assisted cracking, which promoted liberation of large, abrasive debris particles.

With presence of a water layer adsorbed onto polar GaN surface, water molecules can split and form Ga-OH bonds at the surface [42,50].

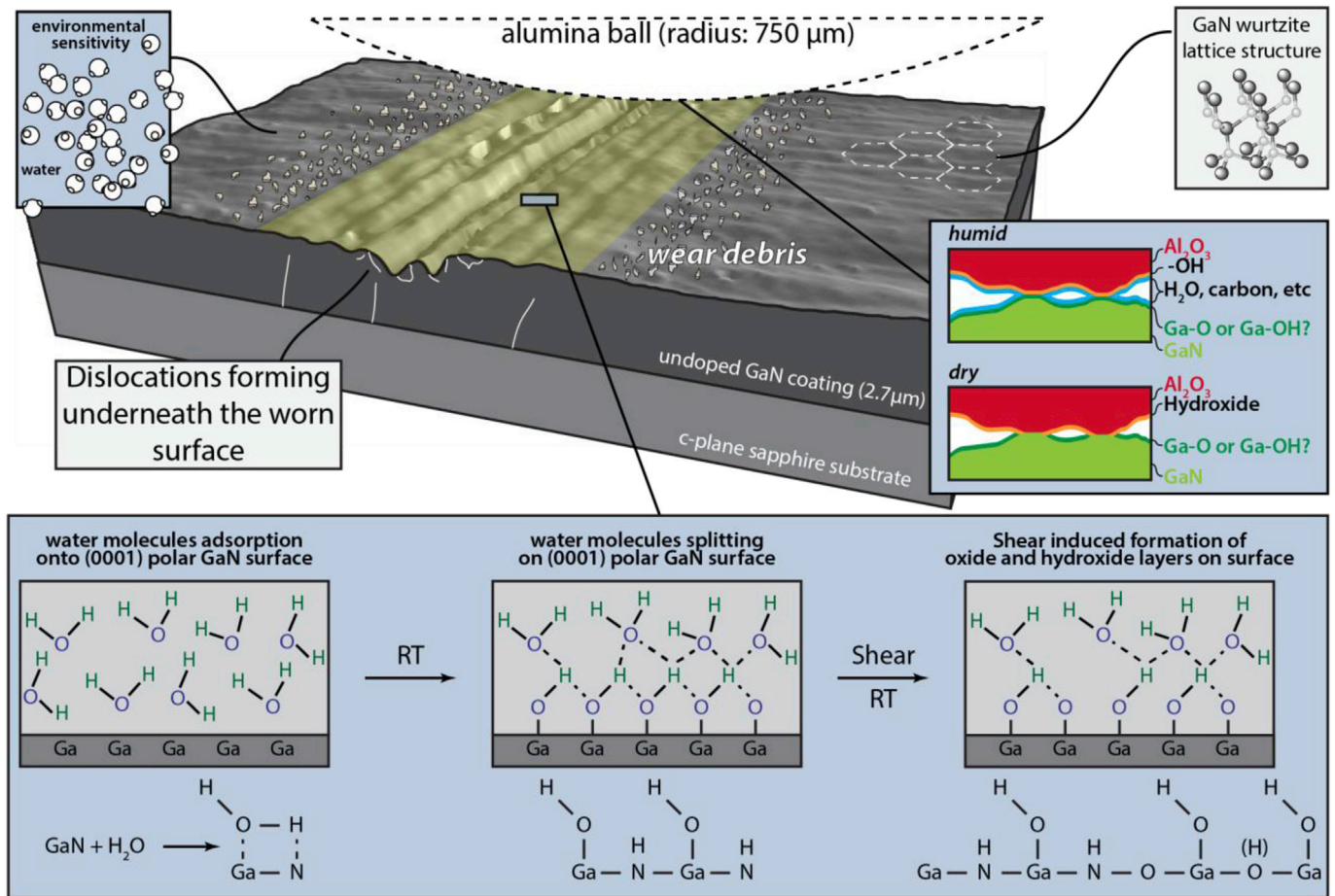


Fig. 9. Illustration of proposed wear mechanism of GaN under humid environments [42,50].

We hypothesize that applied shear stress at the interface between water and GaN will induce the formation of oxide and hydroxide, which have higher wear rate and can be removed easily as the wear debris (Fig. 9). When comparing the high humidity (75% RH) to low humidity (10% RH), we hypothesize there is a competition between tribochemical oxidation (forming a lubricous, but high wear material) and material removal; when oxidation is faster, there is a thicker average oxide layer and material can be removed quicker. If oxidation is slowed (as in the 10%), the oxide/hydroxide layer remains thin, lubricating the interface and slowing the removal process. Once the wear debris was created, some debris will spread along the sides of and within the wear scar while some will accumulate on the surface of ruby probe and be involved in the following wear process. The multitude of nanometer size wear debris can act as high contact pressure abrasive particles, which in turn facilitate the material removal of the continuously oxidizing sliding surface. In the dry nitrogen environment, tribochemistry with the environment is less likely to occur without the chemisorption of water molecules; the wear process between GaN and ruby countersample in dry nitrogen environment is hypothesized to be dominated by adhesive-type wear. Ridges perpendicular to the wear scar and high friction coefficient support an adhesive wear component. We cannot rule out fatigue-related mechanisms for ejection of larger debris particles from the pot-hole like worn regions.

4. Conclusion

In this study, tribochemistry of GaN under different testing environments were analyzed and the wear mechanism of GaN has been discussed. Wear rate of GaN expanded over two orders of magnitude when tested under different humidity levels. Wear scar obtained under humid

environment has the highest wear rate and moderate friction coefficient. Dry nitrogen environment has the lowest wear rate and highest friction coefficient. The low humidity environment has the lowest and most stable friction during the stable stage and its wear rate is only two time higher than the dry nitrogen environment. SEM/EDS revealed that GaN responded differently to different environments and these were attributed to the difference in GaN wear behavior under different testing environments. More wear debris was found on the ruby probe for the humid testing environment while some material transfers were imaged for low humidity and dry nitrogen environments. This finding together with the AFM scan support the grooving abrasion wear mode in the humid environment and adhesive wear mode in dry nitrogen environment.

Acknowledgements

The authors would like to thank Ronald A. Arif, Wei Sun, and Renbo Song for growing the GaN samples used in this study. The authors would like to thank Greg Sawyer, Nicholas Strandwitz, Christopher Junk, Richard Vinci, Bruce Koel, Xiaofang Yang, Wei Sun and Yiqun Liu for their thoughtful comments and insight. The authors would also like to thank John Angus for his kind explanation of his work to help us better understand the surface chemistry of GaN. The support of the US National Science Foundation [CMMI 1538125] (G. Z. and B. K.), Lehigh University Doctoral Fellowship (G. Z.) and The E. Elmer Klaus Fellowship (G. Z.) are also appreciated. The sample preparation was supported by the U.S. National Science Foundation [ECCS 1408051 and DMR 1505122] (N.T.), and the Daniel E. '39 and Patricia M. Smith Endowed Chair Professorship Fund (N.T.).

References

- [1] Wiederhorn SM. Moisture assisted crack growth in ceramics. *Int J Fract Mech* 1968; 4:171–7. <https://doi.org/10.1017/CBO9781107415324.004>.
- [2] Kimura Y, Okada K, Enomoto Y. Sliding damage of silicon nitride in plane contact. *Wear* 1989;133:147–61. [https://doi.org/10.1016/0043-1648\(89\)90120-8](https://doi.org/10.1016/0043-1648(89)90120-8).
- [3] Ishigaki H, Kawaguchi I, Iwasa M, Toibana Y. Friction and wear of hot pressed silicon nitride and other ceramics. *Trans ASME* 1986;108:514–21.
- [4] Yu J, Chen L, Qian L, Song D, Cai Y. Investigation of humidity-dependent nanotribology behaviors of Si(1 0 0)/SiO₂ pair moving from stick to slip. *Appl Surf Sci* 2013;265:192–200. <https://doi.org/10.1016/j.apsusc.2012.10.168>.
- [5] Yu J, Kim SH, Yu B, Qian L, Zhou Z. Role of tribochemistry in nanowear of single-crystalline silicon. *ACS Appl Mater Interfaces* 2012;4:1585–93. <https://doi.org/10.1021/am201763z>.
- [6] Adachi K, Kato K, Chen N. Wear map of ceramics. *Wear* 1997;203–204:291–301. [https://doi.org/10.1016/S0043-1648\(96\)07363-2](https://doi.org/10.1016/S0043-1648(96)07363-2).
- [7] Eiss NSJ, Fabinak RC. Chemical and mechanical mechanisms in wear of sapphire on steel. *J Am Ceram Soc* 1966;49:221–6.
- [8] Yu B, Gao J, Jin C, Xiao C, Wu J, Liu H, et al. Humidity effects on tribochemical removal of GaAs surfaces. *Appl Phys Express* 2016;9. <https://doi.org/10.7567/APEX.9.066703>.
- [9] Yu B, Gao J, Chen L, Qian L. Effect of sliding velocity on tribochemical removal of gallium arsenide surface. *Wear* 2014;331:59–63. <https://doi.org/10.1016/j.wear.2014.11.026>.
- [10] Fischer TE, Mullins WM. Chemical aspects of ceramic tribology. *J Phys Chem* 1992; 96:5690–701. <https://doi.org/10.1021/j100193a008>.
- [11] Erdemir A, Li S, Jin Y. Relation of certain quantum chemical parameters to lubrication behavior of solid oxides. *Int J Mol Sci* 2005;6:203–18. <https://doi.org/10.3390/i6060203>.
- [12] Murthy VSR, Kobayashi H, Tsurekawa S, Tamari N, Watanabe T, Kato K. Influence of humidity and doping elements on the friction and wear of SiC in unlubricated sliding. *Tribol Int* 2004;37:353–64. <https://doi.org/10.1021/la402856j>.
- [13] Dong X, Jahanmir S. Wear transition diagram for silicon nitride. *Wear* 1993;165: 169–80.
- [14] Yeon J, Van Duin ACT, Kim SH. Effects of water on tribochemical wear of silicon oxide interface: molecular dynamics (MD) study with reactive force field (ReaxFF). *Langmuir* 2016;32:1018–26. <https://doi.org/10.1021/acs.langmuir.5b04062>.
- [15] He H, Qian L, Pantano CG, Kim SH. Effects of humidity and counter-surface on tribochemical wear of soda-lime-silica glass. *Wear* 2015;342–343:100–6. <https://doi.org/10.1016/j.wear.2015.08.016>.
- [16] Gee MG. The formation of aluminium hydroxide in the sliding wear of alumina. *Wear* 1992;153:201–7.
- [17] Perez-Unzueta AJ, Beynon JH, Gee MG. Effects of surrounding atmosphere on the wear of sintered alumina. *Wear* 1991;146:179–96.
- [18] Gee MG, Jennett NM. High resolution characterisation of tribochemical films on alumina. *Wear* 1996;193:133–45. [https://doi.org/10.1016/0043-1648\(95\)06612-8](https://doi.org/10.1016/0043-1648(95)06612-8).
- [19] Sidebottom MA, Pitenis AA, Junk CP, Kasprzak DJ, Blackman GS, Burch HE, et al. Ultralow wear Perfluoroalkoxy (PFA) and alumina composites. *Wear* 2016; 362–363:179–85. <https://doi.org/10.1016/j.wear.2016.06.003>.
- [20] Pitenis A a, Harris KL, Junk CP, Blackman GS, Sawyer WG, Krick BA. Ultralow wear PTFE and alumina composites: it is all about tribochemistry. *Tribol Lett* 2015;57. <https://doi.org/10.1007/s11249-014-0445-6>.
- [21] Sawyer WG, Argibay N, Burriss DL, Krick BA. Mechanistic studies in friction and wear of bulk materials. *Annu Rev Mater Res* 2014;44:395–427. <https://doi.org/10.1146/annurev-matsci-070813-113533>.
- [22] Krick BA, Pitenis AA, Harris KL, Junk CP, Sawyer WG, Brown SC, et al. Ultralow wear fluoropolymer composites: nanoscale functionality from microscale fillers. *Tribol Int* 2016;95:245–55. <https://doi.org/10.1016/j.triboint.2015.10.002>.
- [23] Jacobs TDB, Carpick RW. Nanoscale wear as a stress-assisted chemical reaction. *Nat Nanotechnol* 2013;8:108–12. <https://doi.org/10.1038/nnano.2012.255>.
- [24] Beyer MK, Clausen-schaumann H. Mechanochemistry: the mechanical activation of covalent bonds. *Chem Rev* 2005;105:2921–44.
- [25] Adams HL, Garvey MT, Ramasamy US, Ye Z, Martini A, Tysoe WT. Shear induced mechanochemistry: pushing molecules around. *J Phys Chem C* 2015;119:7115–23. <https://doi.org/10.1021/jp512114g>.
- [26] Hertzberg RW, Vinci RP, Hertzberg JL. *Deformation and Fracture Mechanics of engineering materials*. 5th ed. John Wiley & Sons, Inc; 2012.
- [27] Rais-Zadeh M, Gokhale VJ, Ansari A, Faucher M, Theron D, Cordier Y, et al. Gallium nitride as an electromechanical material. *J Microelectromechanical Syst* 2014;23: 1252–71. <https://doi.org/10.1109/JMEMS.2014.2352617>.
- [28] Ambacher O. Growth and applications of group III-nitrides. *J Phys D Appl Phys* 1998;31:2653–710. <https://doi.org/10.1088/0022-3727/31/20/001>.
- [29] Zeng G, Tan CK, Tansu N, Krick BA. Ultralow wear gallium nitride. *Appl Phys Lett* 2016;109:51602. <https://doi.org/10.1063/1.4960375>.
- [30] Xu X, Vaudo RP, Brandes GR. Fabrication of GaN wafers for electronic and optoelectronic devices. *Opt Mater (Amst)* 2003;23:1–5. [https://doi.org/10.1016/S0925-3467\(03\)00051-X](https://doi.org/10.1016/S0925-3467(03)00051-X).
- [31] Aida H, Doi T, Takeda H, Katakura H, Kim SW, Koyama K, et al. Ultraprecision CMP for sapphire, GaN, and SiC for advanced optoelectronics materials. *Curr Appl Phys* 2012;12:S41–6. <https://doi.org/10.1016/j.cap.2012.02.016>.
- [32] Weyher JL, Müller S, Grzegory I, Porowski S. Chemical polishing of bulk and epitaxial GaN. *J Cryst Growth* 1997;182:17–22. [https://doi.org/10.1016/S0022-0248\(97\)00320-5](https://doi.org/10.1016/S0022-0248(97)00320-5).
- [33] Arif RA, Ee YK, Tansu N. Polarization engineering via staggered InGa_N quantum wells for radiative efficiency enhancement of light emitting diodes. *Appl Phys Lett* 2007;91:2005–8. <https://doi.org/10.1063/1.2775334>.
- [34] Zhao H, Liu G, Zhang J, Poplawsky JD, Dierolf V, Tansu N. Approaches for high internal quantum efficiency green InGa_N light-emitting diodes with large overlap quantum wells. *Opt Express* 2011;19:A991–1007. <https://doi.org/10.1364/OE.19.00A991>.
- [35] Caldas PG, Silva EM, Prioli R, Huang JY, Juday R, Fischer AM, et al. Plasticity and optical properties of GaN under highly localized nanoindentation stress fields. *J Appl Phys* 2017;121:125105. <https://doi.org/10.1063/1.4978018>.
- [36] Erickson GM, Sidebottom MA, Curry JF, Ian Kay D, Kuhn-Hendricks S, Norell MA, et al. Paleo-tribology: development of wear measurement techniques and a three-dimensional model revealing how grinding dentitions self-wear to enable functionality. *Surf Topogr Metrol Prop* 2016;4:1–12. <https://doi.org/10.1088/2051-672X/4/2/024001>.
- [37] Chin AH, Ahn TS, Li H, Vaddiraju S, Bardeen CJ, Ning CZ, et al. Photoluminescence of GaN nanowires of different crystallographic orientations. *Nano Lett* 2007;7: 626–31. <https://doi.org/10.1021/nl062524a>.
- [38] Zeng G, Yang X, Skinner CH, Koel BE, Tansu N, Krick BA. Controlling factors of GaN wear. *Tribol Lubr Technol* 2017;7:3:22–8.
- [39] Ye H, Chen G, Niu H, Zhu Y, Shao L, Qiao Z. Structures and mechanisms of water adsorption on ZnO (0001) and GaN (0001). *Surf J Phys Chem C* 2013;117:15976. <https://doi.org/10.1021/jp312847r>.
- [40] Tan OZ, Wu MCH, Chihai V, Kuo J-L. Physisorption structure of water on the GaN polar surface: force field development and molecular dynamics simulations. *J Phys Chem C* 2011;115:11684–93.
- [41] Bermudez VM, Long JP. Chemisorption of H₂O on GaN (0001). *Surf Sci* 2000;450: 98–105.
- [42] Gao F, Chen D, Tuller HL, Thompson CV, Palacios T. On the redox origin of surface trapping in AlGa_N/GaN high electron mobility transistors. *J Appl Phys* 2014;115. <https://doi.org/10.1063/1.4869738>.
- [43] Du YA, Chen Y-W, Kuo J-L. First principles studies on the redox ability of (Ga(1-x)Zn(x))N(1-x)O(x) solid solutions and thermal reactions for H₂ and O₂ production on their surfaces. *Phys Chem Chem Phys* 2013;15:19807–18. <https://doi.org/10.1039/c3cp53091d>.
- [44] Chakrapani V, Pendyala C, Kash K, Anderson AB, Sunkara MK, Angus JC. Electrochemical pinning of the fermi level: mediation of photoluminescence from gallium nitride and zinc oxide. *J Am Chem Soc* 2008;130:12944–52. <https://doi.org/10.1021/ja710999r>.
- [45] Adamson AW. *Physical chemistry of surfaces*. fourth ed. New York: John Wiley; 1982.
- [46] Hino T, Tomiya S, Miyajima T, Yanashima K, Hashimoto S, Ikeda M. Characterization of threading dislocations in GaN epitaxial layers. *Appl Phys Lett* 2000;76:3421–3. <https://doi.org/10.1063/1.126666>.
- [47] Ee YK, Li XH, Biser J, Cao W, Chan HM, Vinci RP, et al. Abbreviated MOVPE nucleation of III-nitride light-emitting diodes on nano-patterned sapphire. *J Cryst Growth* 2010;312:1311–5. <https://doi.org/10.1016/j.jcrysgro.2009.10.029>.
- [48] Bendersky LA, Tsvetkov DV, Melnik YV. Transmission electron microscopy study of a defected zone in GaN on a SiC substrate grown by hydride vapor phase epitaxy. *J Appl Phys* 2003;94:1676–85. <https://doi.org/10.1063/1.1589169>.
- [49] Ning XJ, Chien FR, Pirouz P, Yang JW, Khan MA. Growth defects in GaN films on sapphire: the probable origin of threading dislocations. *J Mater Res* 1996;11: 580–592. doi:10.1557/JMR.1996.0071.
- [50] Zhang X, Ptasinska S. Electronic and chemical structure of the H₂O/GaN(0001) interface under ambient conditions. *Sci Rep* 2016;1–7.
- [51] Nowak R, Pessa M, Suganuma M, Leszczynski M, Grzegory I, Porowski S, et al. Elastic and plastic properties of GaN determined by nano-indentation of bulk crystal. *Appl Phys Lett* 1999;75:2070. <https://doi.org/10.1063/1.124919>.
- [52] Tsai CH, Jian SR, Juang JY. Berkovich nanoindentation and deformation mechanisms in GaN thin films. *Appl Surf Sci* 2008;254:1997–2002. <https://doi.org/10.1016/j.apsusc.2007.08.022>.